Possible identification of zinc-vacancy—donor-impurity complexes in zinc telluride by optically detected magnetic resonance

J. Bittebierre and R. T. Cox

Groupe de Physique des Semiconducteurs, Service de Physique, Département de Recherche Fondamentale (DRF/SPh/PSC), Centre d'Etudes Nucléaires de Grenoble, Boîte Postale 85X, 38041 Grenoble Cédex, France

(Received 3 March 1986)

Application of the optically detected magnetic resonance (ODMR) technique to donor-acceptor recombination luminescence in donor-doped ZnTe crystals shows the presence of two acceptor centers having noncubic symmetry. One of these centers, labeled A_t, has precisely trigonal symmetry C_3. In terms of a spin Hamiltonian for an effective spin $S = \frac{1}{2}$, its g factors are $g_{zz} = 2.664$ and $g_{xx} = g_{yy} \simeq 0$, where z corresponds to a $\langle 111 \rangle$ direction. The other center, labeled A_m, has mirror symmetry C_S, with $g_{zz} = 2.540$ and $g_{xx} \simeq g_{yy} \simeq 0.25$, where the z axis is inclined at $6.7°$ to $\langle 111 \rangle$ in a $\{110\}$ plane. The g factors are interpreted by considering the effect of a low-symmetry crystal field on a $J = \frac{3}{2}$ (Γ_8) hole in ZnTe. Hyperfine splittings of magnitude 190×10^{-4} cm^{-1} for A_t and 180×10^{-4} cm^{-1} for A_m are observed in the ODMR spectra and attributed to interactions with three equivalent or nearly equivalent Te nuclei. Center A_t is observed in chlorine-doped ZnTe; center A_m is observed in aluminum-doped ZnTe and is very likely the acceptor called A_C, known by its bound-exciton line at 2.369 eV. It is proposed that these single-acceptor centers are double-acceptor—single-donor pairs and, more precisely, that the double-acceptor constituent is the zinc vacancy. That is, the trigonal center A_t is $V_{Zn}Cl_{Te}$ and the mirror-symmetry center A_m is $V_{Zn}Al_{Zn}$. If this interpretation is correct, the electronic properties of vacancy centers in ZnTe are remarkably different from those of the well-known V_{Zn}—donor-impurity associates (the "A centers") in ZnSe and ZnS. Whereas the latter centers are very deep centers with large pseudo-Jahn-Teller distortions, centers A_t and A_m in ZnTe are of shallow or intermediate depth, retain the full symmetry of the vacancy-impurity complex, and have unquenched orbital angular momentum. Finally, it is suggested that the detection of zinc-vacancy acceptors in donor-doped ZnTe may help one to understand the difficulty of producing n-type material.

I. INTRODUCTION

Most II-VI compounds (e.g., ZnO, ZnSe, CdS, etc.) are easily made to be n-type conducting whereas they cannot be made p-type. Zinc telluride presents the opposite problem: Crystals of ZnTe are usually p-type as grown, due to the predominance of shallow acceptor impurities, notably Li and Cu.[1,2] As far as we know, all attempts to prepare n-type ZnTe samples by doping with donor impurities have failed. At the most, semi-insulating (that is highly compensated) material is obtained.

As is well known, donor-acceptor recombination luminescence provides a very useful tool for studying donors and acceptors in compensated semiconductors.[3] Also, the application of optically detected magnetic resonance (ODMR) to the D-A luminescence can often provide detailed identifications of the donors and/or the acceptors.[4] We have been using ODMR in order to try to obtain a better understanding of donor-doped ZnTe. Unexpectedly, in this study we discovered two new acceptor centers. This article is concerned with these centers. The centers have noncubic symmetry and we call them A_t and A_m, where t and m designate trigonal and mirror symmetries, respectively. The A_m center may be identical to the acceptor called A_C known by its bound exciton luminescence line at 2.369 eV.[5-7]

According to usual definitions of the term "shallow," the A_t and A_m acceptors appear to be shallow centers (although the central-cell corrections to some of their properties are so large that "intermediate-depth" centers might be a more appropriate term). As such, they form a new class of acceptor centers in II-VI semiconductors because previously identified shallow acceptors in these compounds all have the full symmetry of the crystal lattice sites (that is cubic in zinc-blende compounds, trigonal in wurtzite compounds). We believe that the new centers in ZnTe are *double-acceptor—single-donor* pairs. An obvious model for such a center is then a zinc vacancy—donor impurity pair $V_{Zn}D$, analogous to the well-known "A centers" in ZnS and ZnSe. As will be seen there is strong spectroscopic evidence for such an assignment, in particular, hyperfine interactions which agree with the model involving a vacancy have been observed. If the centers are indeed vacancy centers, then, being shallow or intermediate-depth centers, they have very different properties from those of the A centers in ZnS and ZnSe, which are *deep* centers. This would be of considerable interest in view of the current interest in understanding the transition between shallow centers and deep centers in semiconductors. In addition, the observation of vacancies acting as acceptors and therefore compensating the donor impurities would help to explain the difficulty in preparing n-type ZnTe.

Brief descriptions of our spectra have appeared previ-

©1986 The American Physical Society

ously.[8,9] This paper gives a much more complete account and includes in particular information about the hyperfine structure that leads us to propose a vacancy model.

Our samples were grown by the Bridgman technique at LETI (Laboratoire d'Electronique et de Technologie de l'Informatique), Grenoble, by Schaub.[10] The starting materials were ZnTe doped with (a) $CdCl_2$ (0.25 at. % Cl—Te) and (b) Al_2Te_3 (0.025 at. % Al—Zn). Capacitance-voltage measurements on indium-ZnTe Schottky diodes showed that both types of crystal were semi-insulating with carrier concentrations $< 10^{13}$ cm^{-3}.

II. LUMINESCENCE SPECTRA

A. Cl-doped ZnTe

The luminescence of samples from Schaub's chlorine-doped ZnTe crystals was first studied by Magnea.[11] Near the band-gap energy of 2.39 eV, the samples gave trapped-exciton and donor-acceptor recombination spectra characteristic of shallow acceptors (Li,Cu) and of shallow donors. Magnea concluded that Cl can act as a shallow donor with ionization energy $E_i = 20.1$ meV. He found in addition that these samples give a broad emission band peaking in the infrared at about 760 nm (1.63 eV). The peak position shifted to shorter wavelengths with increasing laser power, suggesting that the emission corresponds to D-A recombination (such shifts result from the mutual dependence of radiative lifetime and Coulomb-interaction energy on the D-A distance[3]). The relatively low energy of the emission implies that either the donors or the acceptors (or both) are deep centers.

It is Magnea's infrared band that concerns us in the present study. Its appearance (as detected with a gallium-arsenide photocathode having flat response to beyond 850 nm) is shown in Fig. 1(a) where it is seen to be about 0.27 eV wide. The spectrum of Fig. 1(a) is a time-resolved spectrum, obtained by using pulsed-laser excitation and gated detection[12] delayed 1.5 ms after the end of
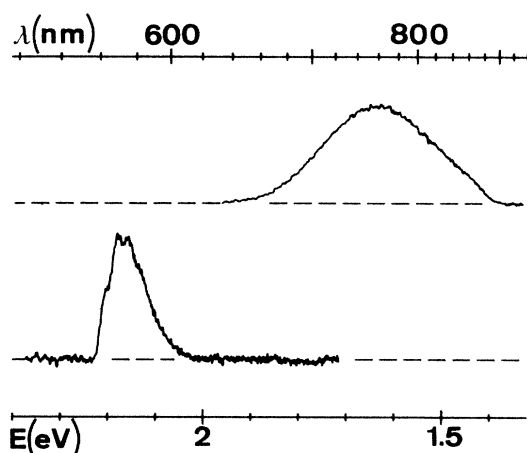

FIG. 1. Luminescence spectra showing the infrared emission band of ZnTe:Cl (upper trace) and the yellow emission of ZnTe:Al (lower trace); $T=2$ K, 514-nm excitation. The spectra were obtained by a time-resolved technique, see the text.

the laser pulse. The band shifts to higher energies if the delay time is reduced and to lower energies if the delay is increased, which again is characteristic of donor-acceptor recombination emission.[3]

B. Al-doped ZnTe

Several authors have reported that Al-doped or Al-implanted ZnTe gives a *yellow* luminescence band.[11,13] We observed a band of this type for Schaub's Al-doped crystals, as illustrated in Fig. 1(b). The figure shows a time-resolved spectrum, taken at short delay time (4 μs after the laser pulse) because the intensity of this band falls off very quickly with increasing time. Again the band shifts with delay time in the way that is characteristic of donor-acceptor recombination.

The band peaks at about 575 nm (2.16 eV), depending on the observation conditions, as noted above. It is relatively narrow (about 0.1 eV wide) and asymmetric. In Fig. 1(b) it shows partly resolved phonon structure with the zero-phonon line at about 2.20 eV. The emission energy is relatively close to the band-gap energy (2.39-eV) but at significantly lower energy than the D-A emissions involving lithium and copper acceptors (zero-phonon energies: 2.32 and 2.23 eV, respectively).

III. ODMR MEASUREMENTS

The excited states responsible for these luminescence bands were studied by ODMR. The samples were immersed in liquid helium at about 2 K inside an 8.7-GHz microwave cavity placed in a magnetic field B. The luminescence was excited by 488- or 514-nm argon laser light and observed perpendicular to B through a window in the cavity wall. Our ODMR spectrometer usually runs in a "time-resolved" mode,[14] with pulsed-laser excitation and a gated photo-multiplier (PM) detector operated at a delay time t_D after the end of the laser pulse. Microwave power is applied during alternate detection periods and the microwave-induced delayed luminescence is extracted by lock-in detection. The ODMR spectrum can be studied as a function of the excited state lifetime by varying the cycle rate of the pulse sequence.

A. Cl-doped ZnTe

Figure 2 shows an ODMR spectrum for Cl-doped ZnTe, with the magnetic field B parallel to a $\langle 100 \rangle$ direction. Here the emission wavelengths observed are restricted to the range 620—830 nm by the combination of a red filter and the photomultiplier's infrared cutoff (the PM was an EMI 9816G tube with S20 response,[12] less infrared-sensitive but better adapted to the ODMR work than the GaAs PM used for Fig. 1).

The ODMR spectra observed for Cl-doped ZnTe correspond to two distinct paramagnetic centers. One of these gives a complex pattern of lines centered at $g=1.96$ (0.32 T), whose appearance changes only slightly with magnet-field orientation. This spectrum was first observed by ordinary EPR spectroscopy (that is microwave-detected EPR) under photoexcitation.[15] It was subsequently observed by ODMR at Lehigh University[16] and Grenoble.[8]

It has been attributed to a trigonal-symmetry electron center.[8,15] The complex line pattern (see Fig. 2) corresponds to chlorine hyperfine interaction and the center is thought to be some form of deep donor center involving chlorine and another defect or impurity situated along its trigonal axis. We shall not discuss this center any further here: we will simply refer to it as the "deep chlorine donor center."

We are interested here in a second ODMR spectrum made up of four lines whose field positions vary over a very wide range as the orientation of B is changed with respect to the crystal axes. In Fig. 2, B is oriented along $\langle 100 \rangle$ and the four lines coalesce into a single line at $g = 1.54$ ($B = 0.40$ T); the lines show weak hyperfine satellites on either side which will be discussed later. From the form of the angular dependence, one can attribute the spectrum to a center with spin $S = \frac{1}{2}$ and trigonal symmetry (the four lines corresponding to the four $\langle 111 \rangle$-type sites). We label this center the "A_t center" (t for trigonal). As far as we know it has never been seen by ordinary EPR.

For a given site, the g factor (determined from $h\nu/\mu_B B$, where $h\nu$ is the microwave quantum at resonance, μ_B is the Bohr magneton) appears to obey a particularly simple law:

$$g = g_{||} \cos\theta . \tag{1}$$

Here, θ is the angle between B and the site's trigonal symmetry axis and $g_{||} = 2.66$ (the sign of g is undetermined). Thus the line positions B vary as $1/\cos\theta$: the curves of B against θ have a very broad minimum, then move more and more rapidly to high fields. The lines broaden as θ increases and, at large angles lose intensity so that they cannot be followed beyond about $\theta = 70°$ (0.7 T). We attribute the broadening to the effects of strain: this induces local variations in the orientation of the c axis and the effect on the linewidth increases with $dB/d\theta$.
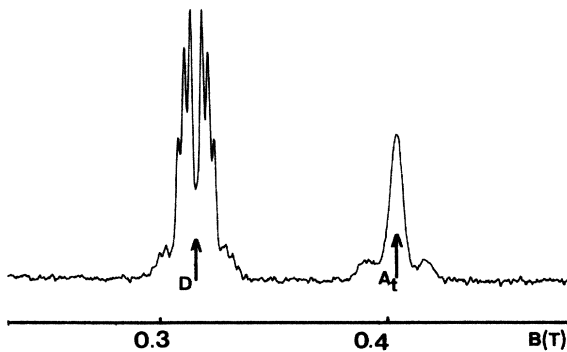

FIG. 2. 8.7-GHz ODMR spectrum (i.e., the microwave-induced intensity change as a function of magnetic field B) obtained via the infrared emission of ZnTe:Cl at 2 K. B is parallel to $\langle 100 \rangle$. Spectrum D corresponds to the deep chlorine donor center (both allowed and forbidden Cl hyperfine transitions are visible as discussed in Ref. 8). Spectrum A_t consists of four lines that coincide exactly for this orientation and corresponds to a trigonal symmetry acceptor.

TABLE I. Principal values of g tensor and values of η (angle of tilt of z axis towards $\langle 110 \rangle$) for centers A_t and A_m. Value of hyperfine interaction constant, A for these centers.

Center	A_t	A_m
g_{zz}^{expt}	2.6636±0.001	2.5402±0.001
g_{yy}^{expt}	0	0.27 ±0.05
g_{xx}^{expt}	0	0.22 ±0.05
η	0°	6.7° ±0.2°
$\|A\|$ (cm^{-1})	192±6×10^{-4}	180±6×10^{-4}

In the range of angles for which the ODMR lines were observable, Eq. (1) was found to be extremely accurate. We checked this equation by orienting B very precisely first along $\langle 111 \rangle$ (to measure $g_{||}$) then along $\langle 100 \rangle$ [to measure g (54.7°)]. The $\langle 100 \rangle$ orientation was achieved to within 1/4° by rotating and tilting the magnet until the four lines coalesced perfectly; the $\langle 111 \rangle$ orientation was achieved to within $\sim 2°$, which is sufficiently precise since $dB/d\theta \sim 0$ near $\theta = 0°$. We found that the $\cos\theta$ law is accurate to within 1 part in 1000 at $\theta = 54.7°$. The accurate value of $g_{||}$ is given in Table I.

Before continuing, we note that Eq. (1) cannot be exactly true for it implies $g_\perp = 0$ in which case the microwave transition rate would disappear for B near the c axis, which is not the case. A more accurate expression for g would be of the form $(g_{||}^2\cos^2\theta + g_\perp^2\sin^2\theta)^{1/2}$. The $\frac{1}{1000}$ accuracy of Eq. (1) at $\theta = 54.7°$ requires that $g_\perp < 0.1$.

As seen in Fig. 2, the A_t center ODMR line has a pair of satellites each with amplitude about 13% of that of the central line. These can be attributed to a hyperfine splitting which, at first sight, appears to correspond to interaction with $I = \frac{1}{2}$ nucleus having abundance about 20% (with the central line corresponding to $\sim 80\%$ abundance $I = 0$ isotopes). The satellites are visible on all four lines at all orientations. Like the line position itself, the splitting ΔB between the two satellites appear to follow at least approximately a $\cos\theta$ law, that is

$$\Delta B \simeq \Delta B(0°)/\cos\theta . \tag{2}$$

This means that the hyperfine splitting measured in energy units (cm^{-1}), $A = g\mu_B \Delta B/hc$, is approximately constant. Because the splitting is not large compared to the linewidth, the accuracy of this statement is about ±5% based on measurements at $\theta = 0°$ and $\theta = 54.7°$. The value of A is given in Table I.

Unfortunately, because of the existence of an unusual set of near coincidences in isotopic ratios, the interpretation of the hyperfine interaction is extremely ambiguous. Three elments, namely, Sn, Pb, and Cd have $I = \frac{1}{2}$ isotopes with total abundances near 20%. The isotopes in question are ^{117}Sn and ^{119}Sn (with total abundance 16.2%), ^{207}Pb (22.6%), and ^{111}Cd and ^{113}Cd (25%). The other isotopes of these elements have $I = 0$. Given the magnitude of the ODMR linewidths, ^{117}Sn and ^{119}Sn would not be distinguished from each other, nor would ^{111}Cd and ^{113}Cd. But, in addition, since the center has trigonal symmetry, a hyperfine interaction with $\sim 8\%$ abundant, $I = \frac{1}{2}$ tellurium nuclei can involve groups of three

nuclei and, providing the interaction is not too anisotropic, such a group could mimic a single $I = \frac{1}{2}$ nucleus of about 20% abundance.

The $I = \frac{1}{2}$ isotopes of Te, with their abundances and magnetic moments are [123]Te (0.9%, $\mu = -0.73\mu_N$) and [125]Te (7.0%, $\mu = -0.88\mu_N$). Again, given the ODMR linewidth, the contributions of [123]Te and [125]Te would be additive since their magnetic moments are very similar.

If the interaction involves three equivalent Te, however, there will be a 1.7% probability that two of the nuclei will have $I = \frac{1}{2}$. This would give rise to additional satellites outside the main spectrum, as shown in Fig. 3. We therefore conducted a search for these additional lines on the low-field side of the A_t line for $\theta \sim 10°$, the orientation that gave the best signal-to-noise ratio. The ODMR spectrum was accumulated for a total of ~ 10 h acquisition time to enhance the signal.

Figure 4 shows the result of this measurement. For comparison we show a simulated spectrum for the three equivalent Te nuclei hypothesis. This was calculated by summing Gaussian lines having amplitudes proportional to the abundances of the tellurium isotopes and having splittings proportional to their magnetic moments. We see first of all that there is excellent agreement between the experimental and calculated intensities for the first satellite. Second, there is strong indication of the presence of the very weak second satellite at the expected position on the low-field side of the first satellite. The weak satellite has approximately the correct amplitude with respect to the $I = 0$ line, that is about 0.4%.

We also searched for the equivalent satellite on the opposite side of the $I = 0$ line. Unfortunately, over all useful orientations, the relevant field region was obscured by the presence of other weak ODMR lines (possibly lines of the A_m center discussed below). This prevented definite confirmation of the three equivalent Te interpretation of the

hyperfine splitting. Nevertheless, we feel reasonably confident in attributing the hyperfine interaction to Te nuclei on the basis of Fig. 4.

As discussed in Sec. V E, it can be shown that the A_t center is a neutral acceptor. Furthermore, as noted earlier (Sec. II), the 760-nm band shifts with time delay in time-resolved luminescence measurements, as is characteristic of donor-acceptor recombination bands. Also, if the time-resolved ODMR experiment is run at high pulse rate, giving short delay times < 25 μs between the laser pulse and the detection period, we observe strong broadening of the ODMR lines of the A_t center and of the deep chlorine center. This is characteristic of time-resolved ODMR spectra obtained via donor-acceptor emission bands and results from the exchange interaction between the trapped electron and the trapped hole.[14,17]

Because of these effects and because we detect both the A_t center and the chlorine center ODMR signals via the 760-nm band, we can attribute this band to the following electron-hole recombination process:

$$D^0_{\text{deep}} + A_t^0 \rightarrow D^+_{\text{deep}} + A_t^- ,$$ (3)

where D_{deep} means the deep chlorine center. We believe that A_t is a shallow or intermediate-depth center so that it must be the considerable depth of the Cl center that pushes the emission into the infrared.
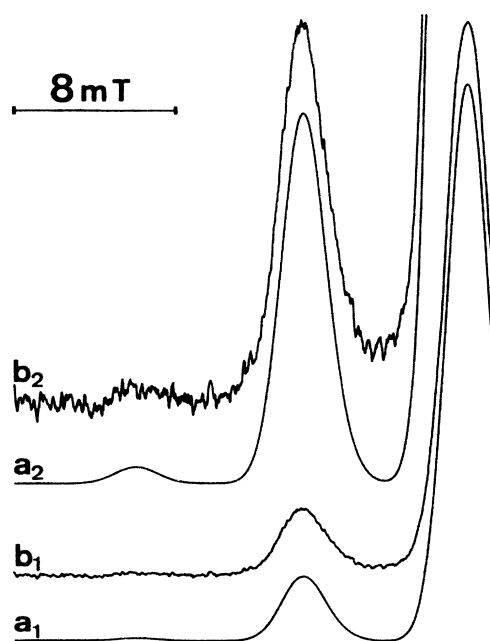
FIG. 4. Low-field side of the A_t center ODMR line for B at $\sim 10°$ to the trigonal axis. Traces a_1 and a_2 are simulated spectra for the case of hyperfine interaction with three equivalent Te; traces b_1 and b_2 show the experimental spectrum. The scale is increased $\times 5.5$ in traces a_2 and b_2. The simulated spectrum is a sum of Gaussian shaped components and is adjusted to fit the $I = 0$ line (line at the right).
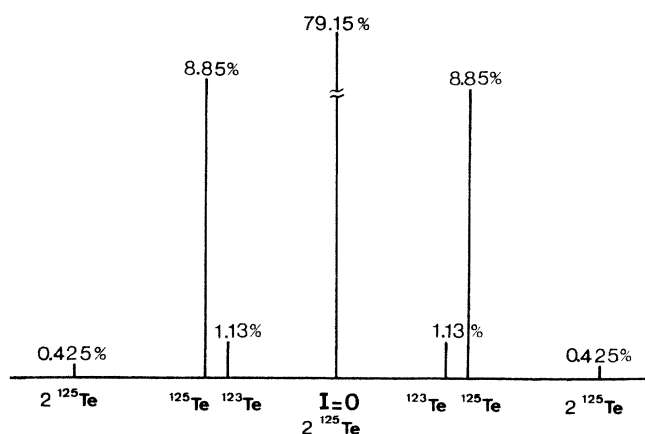

FIG. 3. Relative intensities and positions for the strongest lines in the ODMR (or EPR) spectrum of a spin $S = \frac{1}{2}$ interacting with three equivalent Te. The central line corresponds to the case where all three nuclei are $I = 0$ isotopes; label [125]Te means one nucleus is [125]Te ($I = \frac{1}{2}$) and the other two have $I = 0$; 2 [125]Te means two nuclei are [125]Te and the third has $I = 0$, etc. Many weaker lines (e.g., [125]Te + [123]Te) are not shown.

B. Al-doped ZnTe

Another multiline magnetic resonance spectrum was detected optically via the yellow emission characteristic of ZnTe:Al. This spectrum consists of 12 lines. It resembles the four line spectrum given by the A_t center but each line is now split into three, showing that the symmetry is lower than trigonal. We will attribute this spectrum to another acceptor center which we will call the A_m center because it has mirror symmetry on a $\{110\}$ plane.

Again, we attribute the luminescence to donor-acceptor recombination. However, here the donor must be a *shallow* donor because the emission energy lies close to that of, e.g., the shallow donor-copper-acceptor emission. The emission process is

$$D_s^0 + A_m^0 \rightarrow D_s^+ + A_m^- , \tag{4}$$

where D_s is the shallow donor. No donor ODMR is detected via the yellow emission since shallow donors in ZnTe have $g \sim 0.4$,[18] giving resonance at 1.6 T for 9 GHz, beyond the range of our magnet.

Figure 5 shows measured line positions for B rotating in a $\{110\}$ plane. It is from this kind of splitting pattern that we deduce that the center occupies 12 equivalent mirror symmetry sites. Various sites become degenerate for B parallel to the crystal directions $\langle 100 \rangle$, $\langle 111 \rangle$ or $\langle 110 \rangle$, see Fig. 5. The figure shows that the minimum

line position (maximum g factor) occurs at a field orientation about 7° away from $\langle 111 \rangle$. As in the case of the A_t spectrum, the angular variation curves have very broad minima. The lines broaden when they move off to high field and become undetectable at lower field than in the case of the A_t center because the signal-to-noise ratio is not as good for this spectrum.

The angular variation has approximately the form $B = B_{min}/\cos\theta$, where θ is the angle between the field and the position at which the minimum resonance field, B_{min}, occurs. However, there is now a small detectable deviation from this law, related to the lower symmetry. The accurate g tensor now has three principal values g_{zz}, g_{yy}, g_{xx}, with the later two values small but nonzero. The values, determined from measurements with B parallel to $\langle 111 \rangle$, $\langle 110 \rangle$, $\langle 001 \rangle$, are given in Table I. Unfortunately, the small principal values, g_{yy}, g_{xx}, could not be determined very precisely because in the useful orientation range they contribute very little weight to the g factor $[=(\sum_i g_{ii}^2 \cos^2\theta_i)^{1/2}$ where θ_i is the angle between B and $i = x,y,z]$.

Table I shows that the g tensor is not very different from that of the trigonal acceptor A_t. The value of g_{zz} is very similar and g_{xx}, g_{yy}, although nonzero, are still very small. Instead of being oriented exactly along $\langle 111 \rangle$, the z axis is now tilted away from this direction towards $\langle 110 \rangle$, but η, the angle of tilt is only 6.7°.

Each line in the A_m center spectrum has a pair of satellite lines very similar to those seen on the A_t center lines. This is illustrated in Fig. 6 for the $\langle 110 \rangle$ orientation, where a long accumulation time has been used to improve the signal (the weak, negative-going line seen in Fig. 6 corresponds to an unidentified center which we presume is being detected indirectly via the yellow luminescence). Again, the interaction measured in energy units appears isotropic to within a measurement accuracy of about 10%. The signal-to-noise ratio is not good enough to warrant a search for additional satellites like those discussed in our earlier description of the A_t center's spectrum. However, by analogy, we propose that the hyper-
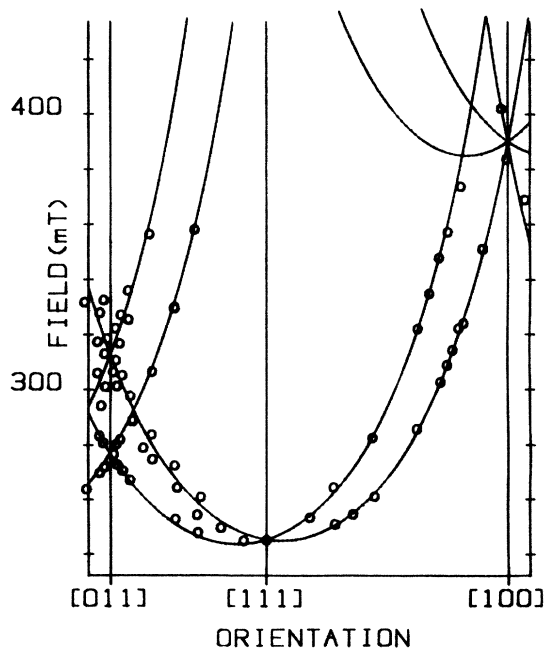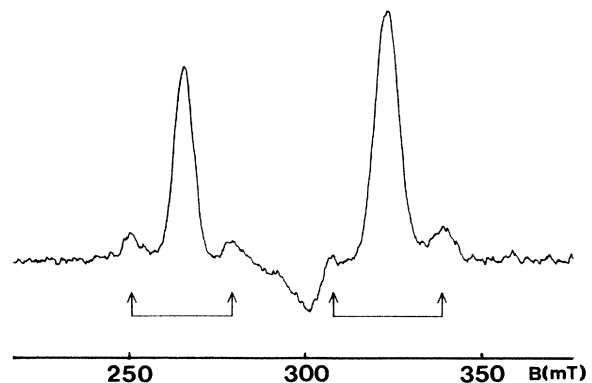

FIG. 5. ODMR line positions for the A_m center as a function of orientation of B at microwave frequency 8.7 GHz. B rotates in a $\{110\}$-type plane. More precisely, the data points were obtained from a rotation scan in a slightly misoriented plane which causes small, extra splittings on the left-hand side whereas the curves are calculated from the g tensors of Table I, which was deduced from the line crossings with B set very precisely along $\langle 011 \rangle$, $\langle 111 \rangle$, and $\langle 100 \rangle$.

FIG. 6. Two of the A_m center's ODMR lines, with hyperfine satellites marked by arrows. The field B is along $\langle 110 \rangle$, microwave frequency is 8.7 GHz, $T = 2$ K. (The negative-going line in center is unidentified.)

fine satellites seen in the A_m spectrum also correspond to three Te nuclei. Note that the nuclei are now only *nearly* equivalent, even if the hyperfine interaction is purely isotropic, since the symmetry is lower than trigonal.

IV. ODMR EMISSION-WAVELENGTH DEPENDENCES

By placing a monochromator in front of the PM detector, one can measure the dependence of the ODMR signal intensity on emission wavelength, thus determining the shape of the emission bands associated with a given ODMR signal. Figure 7 shows results of this kind for ZnTe:Cl. Here, we compare the emission-wavelength dependences of the deep donor and of the A_t center signals with the luminescence spectrum itself, the latter being taken in zero field without applied microwaves.

We see that, within the limits imposed by the rather high noise level (the ODMR signal-to-noise ratio being greatly reduced by the insertion of the monochromator), the emission-wavelength dependence is the same for the chlorine center signal and for the A_t center signal. This is the basis of our assertion [Eq. (3)] that both these centers are involved in a radiative recombination process. The emission-wavelength dependences seem identical to the luminescence spectrum of Fig. 7 except that the latter has an additional shoulder at about 650 nm. Therefore the shoulder must correspond to a quite different emission process [this shoulder moreover is not always present in the luminesence spectra, e.g., it is not seen in Fig. 1(a), and we have not established whether its observation depends on the particular sample or on the excitation or detection conditions].
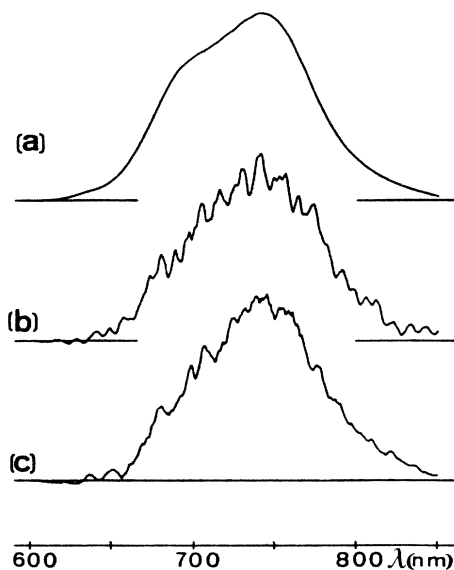

FIG. 7. (a) Infrared emission band of ZnTe:Cl compared with (b) emission wavelength dependence of the A_t center's ODMR signal and (c) emission wavelength dependence of the deep chlorine donor center's ODMR. All three spectra are obtained with an S20 photomultiplier and are uncorrected for wavelength dependence of system sensitivity. $T=2$ K, 514-nm excitation.

For the case of the A_m center, seen in ZnTe:Al, the lower signal levels prevented us from obtaining the emission-wavelength dependence by using a monochromator. However, inserting long-pass optical filters cutting at 560, 580, . . nm, we established that the ODMR signal level dropped out in the same way as the luminescence intensity in this wavelength region. This confirms that the ODMR is associated with the yellow luminescence band of Fig. 1(b), peaking near 575 nm.

Observation of a partly resolved zero-phonon line at about 2.20 eV in Fig. 1(b) enables us to estimate the ionization energy of the A_m acceptor. The energy of the zero-phonon line for donor-acceptor recombination emission is given by $E_G - E_A - E_D + e^2/\epsilon r_{DA}$, where E_G is the band-gap energy, E_A, E_D are the acceptor and donor ionization energies and the last term is the Coulomb interaction between the cores D^+ and A^- separated by distance r_{DA}. We take $E_G = 2.391$ eV and we assume $E_D = 18$ meV (typical for shallow donors in ZnTe). If we guess a value of 15 ± 10 meV for the Coulomb term, then the ionization energy is

$$E_i(A_m) = 188 \pm 20 \text{ meV} .$$

No corresponding estimate can be made for the A_t center's ionization energy but, given the similarity of these two centers, we believe that $E_i(A_t)$ will not be very different.

V. DISCUSSION

A. Origin of the ODMR signal

We have described how magnetic resonance signals for a deep chlorine donor center and the A_t acceptor can be detected as microwave-induced changes of the intensity of the 760-nm band. The ODMR of the A_m acceptor can be obtained via the 575 nm band. Furthermore, both the 760 and 575 nm band show slight shifts towards longer wavelength with increasing time delay in time-resolved luminescence measurements. Such shifts are characteristic of intercenter transitions involving a distance-dependent Coulomb energy change.[3] All this information allows us to attribute these bands to donor-acceptor recombination of the general form $D^0 + A^0 \rightarrow D^+ + A^-$ [Eqs. (3) and (4)].

The numerous discussions of ODMR of D-A systems are then relevant, see, e.g., Refs. 4, 17, and 19. Briefly summarizing such discussions, we simply note that the four Zeeman levels $|M_A\rangle|M_D\rangle$ of the donor-acceptor pair (where $M_A = \pm \frac{1}{2}$ and $M_D = \pm \frac{1}{2}$) can be classed into radiative and nonradiative levels because the electric dipole emission obeys effective-spin selection rules. At resonance, microwave-induced transitions between the Zeeman levels can be detected as changes in luminescence intensity because they change the relative population of these levels.

The success of the present experiments in detecting magnetic resonance for acceptors with unquenched orbital angular-momentum may seem surprising since, at one time, it was thought to be very difficult to observe EPR or ODMR for centers of this type. However, as in several

other recent studies,[19-21] good results are obtained here because these are *low-symmetry* acceptors. For cubic acceptors, the magnetic resonance transitions are subject to strain broadening due to the extreme strain dependence of the Γ_8 sublevels and, in addition, very fast thermalization occurs within these levels because they are strongly coupled to phonons. Both these effects are harmful in ODMR. For example, in a previous study of ZnTe,[18] donor signals were obtained via a donor-to-shallow cubic acceptor emission but no acceptor signals were seen. As discussed below, the symmetry lowering for the A_t and A_m acceptors splits the Γ_8 state leaving the hole in a relatively strain-insensitive doublet with long thermalization time. It is relevant to cite here other cases where shallow acceptor ODMR has been reported, namely (a) in SiC (Ref. 20) and CdS (Ref. 19), where the atom sites in the hexagonal lattice have trigonal symmetry and (b) in GaP under uniaxial stress.[21]

B. Magnetic properties of low-symmetry acceptors

For cubic acceptors in zinc-blende semiconductors, the angular momentum $(l_h = 1)$ and spin $(s_h = \frac{1}{2})$ of the hole are coupled to give a Γ_8 quartet ground state with a higher lying Γ_7 doublet. The splitting of these two states is very large in ZnTe, of the order of the valence-band splitting $=0.9$ eV. Thus the effect of a small low-symmetry crystal field can be considered as a perturbation acting within the four levels of the Γ_8 quartet. In C_3 or C_s (mirror) symmetry, the quartet splits into two doublets which we label $\pm\frac{1}{2}$ and $\pm\frac{3}{2}$, see Fig. 8. As will be seen, the magnetic resonance properties of centers A_t and A_m show that it is the $\pm\frac{3}{2}$ doublet that is the occupied state for these centers.

A magnetic field splits the doublets as represented on the right-hand side of Fig. 8, the splitting being dependent on the orientation of the field. The effects of the low symmetry and of B may be represented by an equivalent Hamiltonian acting in a $J = \frac{3}{2}$ basis:
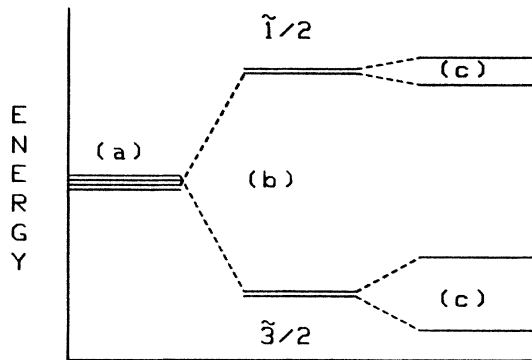

FIG. 8. Energy-level diagram appropriate to acceptors A_t and A_m: (a) $J = \frac{3}{2}$ quartet ground state (Γ_8) of a cubic-symmetry acceptor (b) is effect of C_3 or C_s crystal field (states labeled $\frac{1}{2}$ and $\frac{3}{2}$ are exact or approximate eigenstates of J_z). (c) shows effect of a magnetic field.

$$\mathcal{H} = DJ_z^2 + E(J_x^2 - J_y^2) + g\mu_B \mathbf{B}\cdot\mathbf{J} , \tag{5}$$

where the first two terms in (5) represent the C_3 and C_s crystal-field components, respectively, and the third term represents the Zeeman interaction. We neglect here the "cubic" Zeeman interaction involving terms in $g_{\text{cubic}}\mu_B(B_\xi S_\xi^3 + \ldots)$, where $\xi, \ldots$, are the $\langle 001 \rangle$ directions. We are unable to distinguish any effects of this term in our measurements and there is evidence[22,23] that $g_{\text{cubic}} \ll g$ for a hole in ZnTe.

If the Zeeman term is much smaller than the crystal-field term, then for a given doublet $\pm\frac{1}{2}$ or $\pm\frac{3}{2}$ in Fig. 8, the two states can be represented by the eigenstates of a new Hamiltonian for a fictitious *effective spin* $S = \frac{1}{2}$:

$$\mathcal{H} = \mu_B \mathbf{B}\cdot\tilde{g}^{\text{eff}}\cdot\mathbf{S} , \tag{6}$$

where the effective g tensor, $\tilde{g}^{\text{eff}}$, is very anisotropic.

In C_3 symmetry, for the doublet $\pm\frac{3}{2}$, the tensor $\tilde{g}^{\text{eff}}$ is related to the g factor of (5) by $g_\parallel^{\text{eff}} = 3g$ and $g_\perp^{\text{eff}} = 0$, that is

$$g^{\text{eff}} = 3g\cos\theta . \tag{7}$$

The zero value of $g_\perp^{\text{eff}}$ expresses the fact that $B_x J_x$ and $B_y J_y$ have no matrix elements within the states $\pm\frac{3}{2}$ in the C_3 symmetry case. These states remain pure eigenstates $|J_z = \pm\frac{3}{2}\rangle$ of J_z for all field directions provided that $g\mu_B B \ll D$ in (5). As discussed in Sec. III, Eq. (7) was found to be accurate to 1/1000 out to $\theta = 54.7°$ for the A_t center at 9 GHz. This sets a lower limit on the crystal-field splitting $2D$ induced by the term DJ_z^2 of Hamiltonian (5), namely, $|2D| > 2.4$ cm^{-1}. No estimate can be given of the actual value of $2D$.

Inserting $g_\parallel^{\text{expt}}$ for the A_t center from Table I in Eq. (7), we deduce that the "true" value of g for A_t, that is g in the $J = \frac{3}{2}$ Hamiltonian (5), is $2.664/3 = 0.89$. This value is of the order of the known g factors $= 0.6-0.7$ for the cubic symmetry (Γ_8) acceptors Li, Cu, P, etc., in ZnTe as determined from Zeeman or Raman spectroscopy.[23,24] This result constitutes one of the main features on which we base our attribution of the ODMR spectrum to a fairly shallow acceptor rather than to some kind of deep center.

Nevertheless, $g = 0.9$ is significantly larger than the figure $g = 0.6-0.7$ and we attribute this difference to a relatively large central-cell correction for the A_t center as compared to the usual acceptors. Of course, some hole density in the central cell may be needed to explain how the local crystal field that results from the defect geometry can induce a substantial splitting of the Γ_8 state. Also, a relatively large central-cell effect is needed to explain the large hyperfine interaction obtained with three Te nuclei. The latter point is discussed further in Secs. V C and VI.

The A_m center represents a "slightly" C_s symmetry case. For such a case, $E/D \neq 0$ but remains $\ll 1$ in Hamiltonian (5) and the effective g values for the doublet $\pm\frac{3}{2}$ are related to the g factor of (5) by

$$g_{zz}^{\text{eff}} \simeq 3g , \tag{8a}$$

$$g_{xx}^{\text{eff}} \simeq g_{yy}^{\text{eff}} \simeq 3(E/D)g . \tag{8b}$$

Here, we have neglected terms of order $(E/D)^2$.

For the A_m center, our value of g_{zz}^{eff}, (Table I) implies that the $J = \frac{3}{2}$ g value is $g \simeq 0.85$. This is close to the value found for the A_t acceptor. Application of Eqs. (8b) to our data yields an approximate value for the ratio (E/D), namely $(E/D) \sim 0.08$. The small difference between g_{xx}^{eff} and g_{yy}^{eff} in Table I, at the limit of the experimental error, is of the size and sign expected from a more accurate version of (8b).

C. Hyperfine interactions

The hyperfine satellites seen on the A_t center and A_m center ODMR lines represent, to our knowledge, the first observation of hyperfine splitting for an acceptor center having unquenched orbital angular momentum. In this section, we give a formalism for describing the hyperfine spectrum and then we comment on the magnitude of the observed splitting.

To describe the states $|\mathbf{J}, \mathbf{I}\rangle$, where $J = \frac{3}{2}$ and $I = \frac{1}{2}$, we add a hyperfine term and a nuclear Zeeman term to the $J = \frac{3}{2}$, $I = 0$ Hamiltonian (5). The Hamiltonian becomes

$$\mathcal{H} = \mathcal{H}_J + \mathbf{J} \cdot \widetilde{T} \cdot \mathbf{I} + g_n \mu_N \mathbf{B} \cdot \mathbf{I} , \tag{9}$$

where $\mathcal{H}_J$ represents Hamiltonian (5).

The properties of the hyperfine tensor $\widetilde{T}$ are determined by the *local* symmetry at the nucleus, which may be very different from the overall symmetry of the acceptor wave function. Thus, the principal axes of $\widetilde{T}$ can have orientations very different from those of the axes x, y, z that diagonalize the crystal-field term in (9).

We first consider the trigonal symmetry acceptor A_t where, as discussed in Sec. V B, the operators J_x and J_y have no matrix elements within the occupied doublet $|J_z = \pm \frac{3}{2}\rangle$. Thus, hyperfine terms such as, e.g., $J_x T_{xz} I_z$ in (9) have no matrix elements within the states $|J_z = \pm \frac{3}{2}, \mathbf{I}\rangle$ and, since the hyperfine interaction is much too small to mix these states with states $|J_z = \pm \frac{1}{2}, \mathbf{I}\rangle$, we need only retain those hyperfine terms involving J_z, that is $\sum_i J_z T_{zi} I_i$, where $i = x, y, z$. This sum can be written $J_z \mathbf{n} \cdot \widetilde{T} \cdot \mathbf{I}$, where $\mathbf{n}$ is a unit vector parallel to the trigonal axis z.

The direct effect of the magnetic field on the spin $\mathbf{I}$ [the nuclear Zeeman term in (9)] is negligible compared to that of the hyperfine field and so the quantization axis for $\mathbf{I}$ will be fixed parallel to the vector $\mathbf{n} \cdot \widetilde{T}$. This applies for all field orientations and as a result the hyperfine splitting of the energy levels is isotropic, no matter how anisotropic the tensor $\widetilde{T}$ really is. If we transform to the formalism that represents the states $|J_z = +\frac{3}{2}\rangle$ by an effective spin $S = \frac{1}{2}$, the levels are the eigenstates of

$$\mathcal{H} = \mu_B \mathbf{B} \cdot \widetilde{g} \cdot \mathbf{S} + 3 S_z \mathbf{n} \cdot \widetilde{T} \cdot \mathbf{I} , \tag{10}$$

where $g_{\parallel} = 3g$ and $g_{\perp} = 0$, as in (7). The energy levels are

$$E = g_{\parallel} \mu_B \cos\theta B m_S + A m_S m_I , \tag{11}$$

where $m_S = \pm \frac{1}{2}$, $m_I = \pm \frac{1}{2}$, and the parameter $A = 3|\mathbf{n} \cdot \widetilde{T}|$. This is the equation we used to analyze our

data (Sec. III and Table I): it gives hyperfine splitting $\Delta B = A/(g_{\parallel} \mu_B \cos\theta)$ in a field-swept magnetic resonance spectrum.

A similar description applies in the case of the A_m center. This center has symmetry lower than trigonal but $D \gg E$ in (5) so that the acceptor wave functions remain approximate eigenstates of J_z. This means that the hyperfine interaction will be at least approximately isotropic for a wide range of orientations about the z axis for the A_m center, as was observed (see Sec. III B).

Thus, the observation that the hyperfine splittings (measured in energy units) appear to be isotropic for both the A_t and the A_m centers does not necessarily mean that the hyperfine tensors are highly isotropic for these centers.

The hyperfine interaction consists in principal of three components: (a) the contact interaction between the hole spin $\mathbf{s}_h$ and the nuclear spin $\mathbf{I}$, (b) the dipolar interaction between $\mathbf{s}_h$ and $\mathbf{I}$, and (c) the interaction between the hole's orbital angular momentum $\mathbf{l}_h$ and $\mathbf{I}$. We expect that the major contribution to the isotropic part of the hyperfine tensor will come from the contact interaction (a), giving a term proportional to $|\Psi(r=0)|^2$ (the hole density at the nucleus), and that the major contribution to the anisotropy of the tensor will come from the spin-dipolar interaction (b).

Provided that the crystal field is too small to mix substantially the spin-orbit-split states Γ_8 and Γ_7, the operator $\mathbf{s}_h$ can be represented by $(\frac{1}{3})\mathbf{J}$ within the $J = \frac{3}{2}$ Hamiltonians (5) and (9). Thus, for example, the isotropic contact interaction of form a $\mathbf{s}_h \cdot \mathbf{I}$ contributes a term $(a/3)\mathbf{J} \cdot \mathbf{I}$ to $\mathbf{J} \cdot \widetilde{T} \cdot \mathbf{I}$ in (9) and therefore makes a contribution $3(a/3) = a$ to the hyperfine constant A of Eq. (11) and Table I. There is a similar cancellation of two factors $\frac{1}{3}$ and 3 on transforming the dipolar interaction between the true spin $\mathbf{s}_h$ and $\mathbf{I}$ into its contribution to the effective spin Hamiltonian (10). Thus it is A (not $A/3$) that should be used in any comparison with contact and dipolar hyperfine interactions of centers having quenched orbital angular momentum (i.e., centers with $S = \frac{1}{2}$ and $g \simeq g_e = 2$).

Because we have only one measured parameter, A, any such comparison is extremely difficult, and this for two reasons. Firstly, we cannot separate out the interaction between the orbital angular momentum and the nuclear spin. This is comparable with the spin-dipolar interaction for an orbitally degenerate, isolated atom. It may be much smaller if the three Te interpretation of the hyperfine spectrum is correct, since the degeneracy of the $5p$ orbitals occupied by the hole on the three Te atoms in the acceptor core (see later) would be lifted by the core potential. But even if we can ignore the orbital interaction, we cannot separate the contact and spin-dipolar interactions from each other. For nearly pure-spin centers with cylindrical hyperfine tensors (case of an unpaired electron in an sp hybrid orbital), the contact and dipolar interactions are deduced directly from the trace $(A_{\parallel} + 2A_{\perp})/3$ and the anisotropy $(A_{\parallel} - A_{\perp})$ of the tensor, respectively. In our case, if the $(J = \frac{3}{2})$ hyperfine tensor is cylindrical with principal values $T_{\parallel}$ and $T_{\perp}$ and if the axis for $T_{\parallel}$ is inclined at an angle α with respect to the z axis of Hamil-

tonian (5), we can only say that our constant

$$A = 3(T_{\parallel}^2\cos^2\alpha + T_{\perp}^2\sin^2\alpha)^{1/2}$$

lies somewhere between $3T_{\parallel}$ and $3T_{\perp}$.

Nevertheless, on the assumption that the hyperfine interaction is with three ^{125}Te nuclei, it is instructive to compare our values of A with values of ^{125}Te interactions measured by EPR spectroscopy[25,26] for a particular family of paramagnetic centers in ZnTe, the Zn-site double donors Ge, Sn, Pb. In their singly ionized charge state M^+ (where M represents Ge, Sn or Pb), these are deep centers having $S = \frac{1}{2}$ and $g \simeq 2$.

The electronic structure of the centers M^+ has the following peculiarity: because the impurity site is positively charged there is a strong transfer of electronic density from the four Te ligands on to the impurity. If the wave function of the singly ionized donor is considered to be a mixture of two configurations, namely, M_{Zn}^+ $(Te_4)^0$ and $M_{Zn}^0(Te_4)^+$ [where $(Te_4)^+$ means a hole in a molecular orbital shared by the four ligands], there is about 70–80 % of the second configuration.[25] Therefore, the Te hyperfine interactions in these centers can serve as reference values, giving the magnitude of the interactions to be expected for a highly localized hole in ZnTe. Averaging the data for the Ge^+, Sn^+, and Pb^+ centers, the principal values of the hyperfine tensors are

$$A_{\parallel} = -287\times10^{-4}\ cm^{-1}, \quad A_{\perp} = -85\times10^{-4}\ cm^{-1}$$

for each ligand. If the molecular orbital (Te_4) is constructed from Te $5s$ and $5p$ atomic orbitals, then the trace $(A_{\parallel}+2A_{\perp})/3$ is the contact interaction $g_e\mu_B g_n\mu_N(8\pi/3)\,|\,5s(r=0)\,|^2$ of the $5s$ orbital and the anisotropy $(A_{\parallel}-A_{\perp})$ is the dipolar interaction $(\frac{6}{5})g_e\mu_B g_n\mu_N/\langle 5p\,|\,r^{-3}|5p\rangle$ of the $5p$ orbital (this neglects core polarization in the $5p$ orbital and a small orbital contribution to the hyperfine interaction). Then taking values of $|\,5s(r=0)\,|^2$ and $\langle 5p\,|\,r^{-3}\,|\,5p\rangle$ from theoretical Te-atom wave functions gives the relative weights of the two orbitals in the $(MTe_4)^+$ centers to be about 4% $5s$ and 96% $5p$.[25]

We suppose that the wave function of the hole in our acceptor centers A_t and A_m can be represented very crudely as a sum

$$\Psi = c_1\Psi_{core} + c_2\Psi_{exp} \qquad (12)$$

with $c_1^2 + c_2^2 = 1$. Here Ψ_{core} is a normalized molecular orbital (of A_1 symmetry in the point group of the defect) localized on three Te nuclei in the core region and Ψ_{exp} is a normalized, delocalized function falling off exponentially with distance (the product of a spherical, exponential envelope function and a valence band-edge Bloch function). Then an approximate measure of the weight c_1^2 of the Te_3 molecular orbital in the wave function Ψ is given by the ratio of the hyperfine interactions in the acceptor centers to the values cited above for the $(MTe_4)^+$ centers [or, more precisely, by this ratio $\times\frac{3}{4}\times0.75$, because there are three nuclei instead of four and because the hole is only about $\sim75\%$ localized on the ligands in $(MTe_4)^+$].

Because of the problems mentioned earlier and because

a small change in hybridization, increasing the $5s$-orbital contribution, could increase the contact interaction and the trace of the hyperfine tensor very markedly, we can draw no precise conclusions. However, it is remarkable that the values of A in Table I (192×10^{-4} and 180×10^{-4} cm^{-1} for the A_t and A_m centers, respectively) are of the same order as the values of $|\,A_{\parallel}\,|$ and $|\,A_{\perp}\,|$ listed above for the $(MTe_4)^+$ centers. This requires that the hole wave function have a high density in the acceptor core.

For example, if we make the extreme, simplifying assumption that the ratio of $5s$ to $5p$ is the same as it is in the $(MTe_4)^+$ centers, we can fix the ratio $T_{\parallel}/T_{\perp}$. If we further assume that the $5p$ orbitals are oriented at an angle $\alpha = 109°$ to the z axis, as might be appropriate for the defect models discussed in Sec. VI (Fig. 10), we can fix the symmetry axis of $\bar{T}$ at this angle. Then the values of $3T_{\parallel}$ and $3T_{\perp}$ are extractable from the value of A in Table I and the above comparison procedure leads to a value of 0.9 for c_1^2 in Eq. (12) for the A_t center.

Clearly, the assumptions just made cannot be justified. Also 0.9 is an absurdly high value for the weight of Ψ_{core} in the acceptor wave function, Eq. (12), because then we would not have a shallow-acceptor-like g tensor, which requires a large weight of the component Ψ_{exp} involving the orbitally degenerate Bloch function. However, we conclude that a large fraction of the hole wave function is localized on three Te atoms in the core of the acceptor centers A_t and A_m. So from this point of view the term "shallow" acceptor may not be a very appropriate description of these centers.

D. Comparison with the C acceptor

We now compare our data for A_m with the properties of a center called the "C acceptor" or A_C, which gives a characteristic bound-exciton recombination line at 523 nm (2.369 eV). Extensive studies of this line under magnetic field[5,6] and uniaxial stress[7] have shown that A_C is a single acceptor (that is a center with one hole) and that it has noncubic symmetry. (In the first Zeeman work,[5] due to the limited resolution, the symmetry was thought to be trigonal; however, the subsequent stress-splitting studies showed clearly that the symmetry is mirror symmetry.)

De Maigret[7] has analyzed his stress-splitting data in terms of a $J = \frac{3}{2}$ Hamiltonian for C_s symmetry, identical to the crystal-field part of our Hamiltonian (5). He concluded that (a) the z axis is tilted a small angle $\eta \sim 10°$ away from $\langle 111\rangle$ toward $\langle 110\rangle$ and that (b) the E/D ratio is about 0.1–0.2. Furthermore, the Zeeman data[5] (analyzed at the time in terms of a trigonal model, but this would introduce little error since η is small) gave $g_{zz}^{eff}\simeq2.7$ and $g_{xx}^{eff}\sim g_{yy}^{eff}\sim0$.

The similarity of all of these results and our ODMR data for the A_m center is striking

	g_{zz}	η	E/D
A_C center	2.7	10°	0.1–0.2
A_m center	2.54	6.7°	~0.08

(Note that the angle of tilt is in the same direction for the two centers.) The differences are all within the estimated

experimental errors. Furthermore, aluminium doping is known to enhance the A_C bound-exciton luminescence.[27]

Therefore, our acceptor A_m is almost certainly the C acceptor. If it is not, it must be a very closely related center.

E. Atomic models

It is well established that the acceptor A_C is a *neutral, single* acceptor (the excited states of the exciton trapped by A_C fit the "donorlike" model[6] which would only be true if A_C itself has a single hole and is neutral). Given the similarity between the properties of the three acceptors A_C, A_m, A_t (and remembering that A_C and A_m are probably the same center), we will assume that they are all neutral, single acceptors.

An obvious model for a low-symmetry, neutral single acceptor is a *double-acceptor—single-donor* pair. That is, the neutral center would be an $A^{2-}D^+$ core plus a bound hole. We proceed now to develop a detailed model on the basis of this hypothesis.

We recall that the acceptor A_t has precisely trigonal symmetry. Unless we introduce models involving atoms in interstitial sites, there is only one reasonable model giving this symmetry, namely, a nearest-neighbor associate. That is, we locate one component of the AD pair on a Zn site and the other on one of the four Te sites along the $\langle 111 \rangle$ directions. This is illustrated on the left-hand side of Fig. 9.

The A_m acceptor has C_s symmetry. A simple C_s symmetry model is obtained by placing D and A on second-nearest-neighbor sites, i.e., on the same sublattice, as shown on the right-hand side of Fig. 9. Or, in a less obvious model (not illustrated in Fig. 9), we could keep D and A on nearest-neighbor sites but allow either D or A to move off center.

A priori, the double-acceptor component A in Fig. 9 could occupy either the Zn site or the Te site. To form a double acceptor requires lowering the valence at a lattice site by two units. For the zinc site, this reduces the valence to zero so the only obvious Zn-site double acceptor is the *vacancy* V_{Zn}. On the Te site, the obvious double acceptors would be the group-IV elements C, Si, Ge, Sn, Pb.

There is little previous knowledge to help us distinguish between the two possibilities. Nothing is known about possible shallow- or intermediate-depth states of the zinc vacancy since the identified metal-vacancy centers in II-VI compounds are all *deep* centers (see Sec. VI). Nor is it established whether group-IV impurities can occupy the nonmetal site in II-VI compounds and thus act as acceptors, although there is currently a certain interest in the possibility of this occurring in ZnTe and CdTe.[28] In particular, a donor—Si_{Te} acceptor pair was proposed as a model for the A_C acceptor in Ref. 6, and Si_{Te} has been proposed as a model for a double acceptor in ZnTe responsible for a bound-exciton line labeled A_X.[22,29] However, these models are only suggestions, based on chemical analyses that show Si as a frequent contaminant of ZnTe. As regards the heavy tetravalent atoms $M=$Ge, Sn, Pb, we note that these are frequently found to act as metal-site donors in ZnTe and CdTe, whereas it has never been shown that they can occupy the Te site. We hesitate to reject entirely a Sn_{Te} or a Pb_{Te} model because the hyperfine splittings described in Sec. III appeared at first sight to correspond to interactions with Sn or Pb isotopes. However, our present opinion is that the vacancy model gives the best explanation of all the data and we will now concentrate on this model.

We first consider the "chemical" evidence that supports the zinc-vacancy model. The A_t and A_m centers are found in ZnTe doped with the donor impurities Cl and Al, respectively. Now vacancy-donor associates $V_{Zn}Cl_{Te}$ and $V_{Zn}Al_{Zn}$ would have trigonal and mirror symmetries, respectively, which is precisely what is required. These two types of vacancy-donor associates are represented in Fig. 10. On the other hand, in the Te-site acceptor model, there is no obvious link with the doping characteristics. A $M_{Te}Cl_{Te}$ associate would have C_s symmetry, instead of the C_3 symmetry observed for the center in ZnTe:Cl, and a $M_{Te}Al_{Zn}$ associate would have C_3 symmetry instead of the required C_s symmetry (unless the Al, being small,
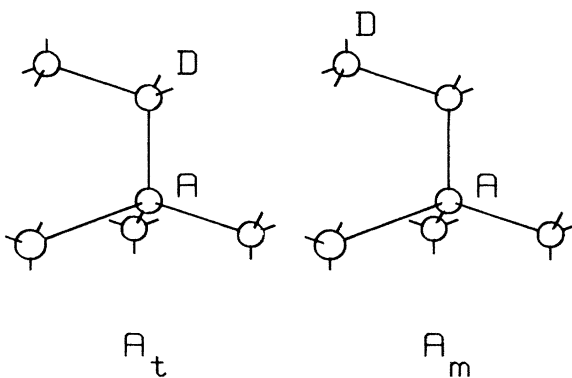

FIG. 9. Two geometrical configurations of a double-acceptor single-donor pair AD in the zinc-blende lattice. Left-hand side configuration has C_3 symmetry as required for an A_t center model; right-hand side arrangement has C_s symmetry as for A_m; *a priori*, the acceptor A could be on either a Zn site or a Te site.
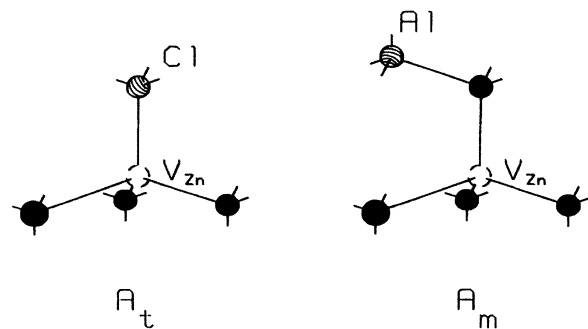

FIG. 10. Proposed models for the A_t and A_m acceptor centers in ZnTe. A Zn vacancy is associated with a Cl impurity on a Te site in the A_t center, with an Al impurity on a Zn site in the A_m center. Black spheres represent Te atoms.

were to go off-center).

Second, we consider the spectroscopic evidence. We recall that the observation of an additional, weak hyperfine satellite strongly suggested that the hyperfine structure corresponded to interaction with three Te nuclei (Sec. III). In an acceptor center, the hole will be localized mainly on tellurium atoms and so we expect a strong hyperfine interaction with the three Te of the base of the tetrahedron containing the vacancy in Fig. 10. These three nuclei would have identical hyperfine tensors in $V_{Zn}Cl_{Te}$ and could well have nearly equivalent tensors in $V_{Zn}Al_{Zn}$ since the Al is far enough away not to render the three nuclei strongly inequivalent. (In $V_{Zn}Al_{Zn}$, there is of course a fourth Te nucleus next to the vacancy, but the neighboring Al^+ donor core will repel the hole-density away from the vicinity of this nucleus.)

Thus, the experimental results strongly support the conclusion that the low-symmetry acceptors found in donor-doped ZnTe are zinc-vacancy—donor-impurity associates, although we cannot entirely rule out other models, in particular complexes involving Sn_{Te} or Pb_{Te}.

VI. IMPLICATIONS OF THE $V_{Zn}D$ MODEL

If it is correct, the vacancy model has very surprising implications because the electronic properties of the vacancy in ZnTe would then be very different from those of equivalent defects in ZnS and ZnSe. In this section we discuss these implications (evidently, if it were to be shown at a later date that the model is false, the comments in this section become null and void).

Defects of type $V_{Zn}D$, where D is a group-VII donor (Cl,Br, etc.) or a group-III donor (Al, etc.) have been known in zinc sulphide and zinc selenide for a long time. These centers, called "A centers," were initially identified[30] by their EPR spectra. It was found that the A centers were implicated in the "self-activated" luminescence[31] of ZnS and ZnSe. ODMR experiments[32] finally proved that the self-activated luminescence is a D-A—type emission resulting when the electron of a distant shallow donor recombines with the hole on the $V_{Zn}D$ complex

The results of this very large body of work on ZnS and ZnSe show clearly that the A centers in these compounds are very deep centers, that is that the hole is strongly bound and very highly localized. In fact, it is localized to the maximum extent possible, being concentrated on to just one of the S or Se atoms neighboring the vacancy. In an ionic model of the crystal, this extreme localization converts an S^{2-} or Se^{2-} ion to an S^- or Se^- ion. The localization on a single atom, which lowers the symmetry of the center below that of the trapping defect, is considered to be a manifestation of the pseudo-Jahn-Teller effect.[33] It can be viewed as a polaronic effect, that is the localized hole is a trapped "small polaron."[34]

A very important consequence of the high localization of the hole and of the additional symmetry lowering in the ZnS, ZnSe A centers is that the orbital angular momentum of the hole is strongly quenched. This leaves

a state which is, to first order, a "pure-spin" state, that is one with g factors near the free-spin value $g = 2$.

Nothing of the kind appears to occur in ZnTe if centers A_t and A_m are identified as analogues of the A centers (and if an early attribution of an A-type center in ZnTe is excluded[35]). First, the A_t and A_m centers are clearly very much shallower than the A centers in ZnS and ZnSe. Secondly, the hole retains the full C_3 symmetry of the trapping defect $V_{Zn}^{2-}Cl^+$ in the A_t center and is approximately uniformly distributed over three Te atoms in the A_m center.

We consider A_t and A_m to be relatively shallow acceptors rather than deep centers for several reasons. Firstly, the ionization energy of the A_m center (deduced from the energy of the yellow emission), $E_i \simeq 190$ meV, is comparable to that of copper ($E_i = 149$ meV), which is usually considered to be a shallow acceptor in ZnTe. Also, the yellow emission band is narrow (~ 0.1 eV wide), that is the phonon coupling is weak. Finally, the g factors of both A_t and A_m centers seem appropriate to the shallow-acceptor theory (Sec. V B).

On the other hand, our acceptor centers are clearly not hydrogenic acceptors. The ionization energy $E_i \simeq 0.2$ eV is considerably higher than that of acceptors considered to be nearly hydrogenic (e.g., lithium, with $E_i = 61$ meV). Also (see Sec. V B), the $J = \frac{3}{2}$ g factors are different from those of hydrogenic acceptors and (see Sec. V C) the large ^{125}Te hyperfine interactions imply that the hole wave function has a density much higher than the hydrogenic value in the core region. Thus, it could be more correct to consider the A_t and A_m centers to be of intermediate depth, that is centers whose properties are considerably modified by core corrections.

Nevertheless, these centers are in no way comparable with the A centers in ZnS and ZnSe, which give very broad (that is strongly phonon-coupled) emission bands at energy far below the band-gap energy. We suggest two reasons for the unusual properties of the A centers in ZnTe compared to those of previously known A centers.

Firstly, because ZnTe is less ionic than ZnS and ZnSe, there will be less interaction between the positive charge of localized hole and distortions of the surrounding shells of metal and nonmetal atoms. That is the strength of the polaronic coupling, tending to localize the hole on to a single atom, is reduced. In Schirmer's description,[34] it is this coupling that drives the pseudo-Jahn-Teller distortion.

Secondly, spin-orbit interaction is very strong in the telluride (as demonstrated by the large spin-orbit splitting of the valence band: 0.9 eV). A pseudo-Jahn-Teller distortion would need to mix states split by the spin-orbit interaction, so this interaction may help to stabilize the vacancy against the distortion.

It has been suggested (e.g., Refs. 36 and 37) that the pseudo-Jahn-Teller distortion contributes a large fraction of the phonon coupling of the recombination emission and a large fraction of the hole-binding energy for zinc-vacancy centers in ZnS and ZnSe. Thus, in conclusion of these comments, we suggest that it is not surprising if the absence of such a distortion in the ZnTe case leaves a much shallower level with only weak-phonon coupling.

VII. CONCLUSION

A considerable amount of information has been obtained about the magnetic and optical properties of these new and interesting acceptor centers, A_t and A_m, in zinc telluride. The data obtained has led us to suggest zinc-vacancy donor-impurity associates as models for these centers. Further work is needed to give a definite proof of these models. In particular, optically detected electron-nuclear double resonance (ODENDOR) experiments of the type described in Ref. 14 could be very helpful for learning more about the hyperfine interactions, but present serious technical difficulties.

The implications of our models for the electronic structure of the zinc vacancy in ZnTe have been discussed in detail in Sec. VI. We note in conclusion that the proposed identification of zinc-vacancy centers in donor-doped ZnTe could be of importance in understanding the chemistry of this compound. It suggests that part of the difficulty in producing n-type ZnTe may be due to compensation by zinc vacancies acting as acceptors. (This idea was common at one time but fell into disfavor when it was shown that the emission bands once attributed to vacancies actually correspond to the acceptor impurities lithium and copper.) As is well known, appropriate reducing treatments can remove the vacancies that compensate the donors in ZnS and ZnSe, so it could be worthwhile reexamining the possibility that similar treatments could convert donor-doped ZnTe to n type.

[1]P. J. Dean, H. Venghaus, J. C. Pfister, B. Schaub, and J. Marine, J. Lumin. **16**, 363 (1978).

[2]N. Magnea, D. Bensahel, J. L. Pautrat, and J. C. Pfister, Phys. Status Solidi B **94**, 627 (1979); J. L. Pautrat, N. Magnea, and J. P. Faurie, J. Appl. Phys. **53**, 8668 (1982).

[3]P. J. Dean, Prog. Solid State Chem. **8**, 1 (1973).

[4]See, e.g., reviews by R. T. Cox, Rev. Phys. Appl. **15**, 653 (1980); J. J. Davies, J. Cryst. Growth **72**, 317 (1985); in *Proceedings of Second International Conference on II-VI Compounds, Aussois,* edited by Y. Marfaing, R. Triboulet, B. Lunn, and J. B. Mullin (North-Holland, Amsterdam, 1985).

[5]J. L. Dessus, Le Si Dang, A. Nahmani, and R. Romestain, Solid State Commun. **37**, 689 (1981).

[6]Le Si Dang, A. Nahmani, and R. Romestain, Solid State Commun. **46**, 743 (1983).

[7]F. de Maigret, thesis, Université Scientifique et Médicale de Grenoble, Grenoble 1984 (unpublished).

[8]K. Saminadayar, R. T. Cox, D. Galland, and Le Si Dang, Physica **116B**, 514 (1983).

[9]J. Bittebierre, R. T. Cox, and K. Saminadayar, J. Cryst. Growth **72**, 332 (1985).

[10]B. Schaub, J. Gallet, A. Brunet-Jailly, and B. Pelliciari, Rev. Phys. Appl. **12**, 147 (1977).

[11]N. Magnea, thesis, Université Scientifique et Médicale de Grenoble, 1982 (unpublished); N. Magnea, K. Saminadayar, D. Galland, J. L. Pautrat, and R. Triboulet, Extended Abstracts of the 159th meeting of the Electrochemical Society, Minneapolis, 1981 (unpublished), p. 404.

[12]The photomultiplier having a GaAs cathode was an RCA C31034 tube, gated by switching the first dynode between its normal operating voltage and $V_k - 15$ V (V_k =cathode potential). This protected the anode during the laser pulses but gave a contrast ratio of only $\sim 30/1$ so an analogue gate was added in the signal channel. The PM with an S20 cathode was an EMI 9816G tube. This could be gated with contrast ratio better than $10^3/1$ by switching the focussing electrode from V_{d1} (first-dynode potential) to $V_k - 15$ V and additional analogue gating was unnecessary.

[13]B. L. Crowder and G. D. Pettit, Phys. Rev. **178**, 1235 (1969); T. L. Larsen, C. F. Varotto, and D. A. Stevenson, J. Appl. Phys. **43**, 172 (1972); M. Quillec, thesis, Université Scientifique et Médicale de Grenoble, Grenoble, 1975 (unpublished).

[14]D. Block, A. Hervé, and R. T. Cox, Phys. Rev. B **25**, 6049 (1982).

[15]K. Saminadayar, D. Galland, N. Magnea, J. L. Pautrat, and R. Triboulet, Phys. Rev. **26**, 2095 (1982).

[16]35-GHz ODMR spectra obtained by Le Si Dang, G. D. Watkins, and K. M. Lee (unpublished).

[17]R. T. Cox, J. J. Davies, and R. Picard, in *Proceedings of the 17th International Conference on Physics of Semiconductors,* edited by J. D. Chadli and W. A. Harrison (Springer, New York, 1985), p. 651.

[18]N. Killoran, B. C. Cavenett, and P. J. Dean, Solid State Commun. **38**, 739 (1981).

[19]J. L. Patel, J. E. Nicholls, and J. J. Davies, J. Phys. C **14**, 1339 (1981).

[20]Le Si Dang, K. M. Lee, and G. D. Watkins, Phys. Rev. Lett. **45**, 390 (1980).

[21]K. M. Lee, thesis, Lehigh University, Bethlehem, 1983 (unpublished).

[22]P. J. Dean, M. J. Kane, N. Magnea, F. de Maigret, Le Si Dang, A. Nahmani, R. Romestain, and M. S. Skolnick, J. Phys. C **18**, 6185 (1985).

[23]H. Tews, Solid State Commun. **34**, 611 (1980); K. Douglas, S. Nakashima, and J. F. Scott, Phys. Rev. B **28**, 846 (1983).

[24]D. J. Toms, J. F. Scott, and S. Nakashima, Phys. Rev. B **19**, 928 (1979).

[25]A recent account of Ge$^+$, Sn$^+$, and Pb$^+$ in ZnTe and CdTe is given by G. Brunthaler, W. Jantsch, U. Kaufmann, and J. Schneider, Phys. Rev. B **31**, 1239 (1985).

[26]K. Suto and M. Aoki, J. Phys. Soc. Jpn. **22**, 1307 (1967); **24**, 955 (1968); T. Iida, J. Phys. Chem. Solids **33**, 1423 (1972).

[27]N. Magnea and R. Romestain (private communications).

[28]J. L. Pautrat, J. M. Francou, N. Magnea, E. Molva, and K. Saminadayar, J. Cryst. Growth **72**, 194 (1985); in *Proceedings of Second International Conference on II-VI Compounds, Aussois* (Ref. 4). This article reviews and tabulates data for donors and acceptors in ZnTe and CdTe.

[29]N. Magnea, J. L. Pautrat, Le Si Dang, R. Romestain, and P. J. Dean, Solid State Commun. **47**, 703 (1983).

[30]For example, J. Schneider, in *II-VI Semiconducting Compounds,* edited by D. J. Thomas (Benjamin, New York, 1967), p. 40.

[31]For example, G. D. Watkins, Solid State Commun. **12**, 589 (1973).

[32]J. R. James, J. E. Nicholls, B. C. Cavenett, J. J. Davies, and D. J. Dunstan, Solid State Commun. **17**, 969 (1975); J. E. Nicholls, J. J. Davies, B. C. Cavenett, J. R. James, and D. J. Dunstan, J. Phys. C **12**, 361 (1979); D. J. Dunstan, J. E. Nicholls, B. C. Cavenett, and J. J. Davies, *ibid.* **13**, 6409 (1980).

[33]For example, F. S. Ham, in *Electron Paramagnetic Resonance*, edited by S. Geschwind (Plenum, New York, 1972), p. 1 (see especially p. 106ff).

[34]O. F. Schirmer, Solid State Commun. **18**, 1345 (1976). An important aspect of Schirmer's approach (originally developed to treat acceptors in highly ionic, octahedrally coordinated oxides) is that the distortion is viewed as a polarization of the shells of ions surrounding the chalcogen site on which the hole localizes. In this view, theories of the zinc vacancy in ZnS and ZnSe that consider only the distortion of the four S or Se surrounding the vacancy cannot succeed; at the very least the Zn atoms of the second shell must be included.

[35]An ESR spectrum for ZnTe, with $g_1 = 2.045$, $g_2 = 2.088$, and $g_3 = 2.091$ was attributed to a deep aluminum A center (that is $V_{Zn}Al$) by R. S. Title, G. Mandel, and F. F. Morehead, Phys. Rev. **136**, A300 (1964). However, the g factors (in particular the fact that no value is smaller than $g_e = 2.0023$) do not fit the pattern now well established by a large body of work on zinc vacancy centers in ZnS and ZnSe.

[36]K. M. Lee, Le Si Dang, and G. D. Watkins, in *Defects and Radiation Effects in Semiconductors 1980*, edited by R. R. Hasiguti (IOP Series 59), (IOP, London, 1981), p. 353.

[37]K. M. Lee, K. P. O'Donnell, and G. D. Watkins, Solid State Commun. **41**, 881 (1982).